

pubs.acs.org/JACS Article

Molecular Z-Scheme for Solar Fuel Production via Dual Photocatalytic Cycles

Pooja J. Ayare, Noelle Watson, Maizie R. Helton, Matthew J. Warner, Tristan Dilbeck, Kenneth Hanson, and Aaron K. Vannucci



Cite This: J. Am. Chem. Soc. 2022, 144, 21568–21575



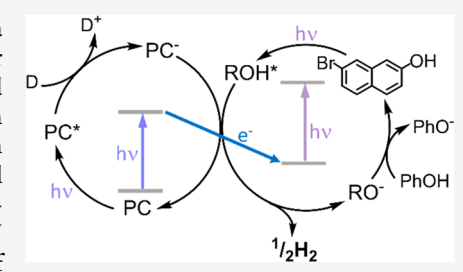
ACCESS I

III Metrics & More

Article Recommendations

Supporting Information

ABSTRACT: Natural photosynthesis uses an array of molecular structures in a multiphoton Z-scheme for the conversion of light energy into chemical bonds (i.e., solar fuels). Here, we show that upon excitation of both a molecular photocatalyst (PC) and a substituted naphthol (ROH) in the presence of a sacrificial electron donor and proton source, we achieve photocatalytic synthesis of H_2 . Data support a multiphoton mechanism that is catalytic with respect to both PC and ROH. The use of a naphthol molecule as both a light absorber and H_2 producing catalyst is a unique motif for Z-scheme systems. This molecular Z-scheme can drive a reaction that is uphill by 511 kJ mol^{-1} and circumvents the high-energy constraints associated with the reduction of weak acids in their ground state, thus offering a new paradigm for the production of solar fuels.



1. INTRODUCTION

The conversion of solar energy into chemical bond energy via photosynthetic organisms is the foundation of life on earth. Given its ubiquity and utility, considerable efforts are underway to realize efficient "artificial" photosynthesis 1-3 that harnesses solar energy for the production of chemical fuels, such as hydrogen (H₂), to meet the energy consumption needs of humans.⁴ Due to the inherent thermodynamic driving forces combined with reaction activation barriers, it is difficult to form chemical bonds with the energy of a single photon that is typically absorbed by photosynthetic chromophores.^{5,6} Nature circumvents this limitation using a Z-Scheme (Figure 1, left), which uses the energies of two photons absorbed at P860 and P700 photocatalysts, for example, to drive chemical bond breaking/making.^{7,8} Two independent excitation events and electron transfer between the photocatalysts enable the generation of strong redox active species that can catalyze the oxidation of water and the reduction of NADP+, a reaction with a of $\Delta G^{\circ} = 220 \text{ kJ mol}^{-1.4,9}$

Artificial photosynthetic systems for solar fuels production (e.g., splitting water into H_2 and O_2 ; $\Delta G^{\circ} = 237$ kJ mol⁻¹) have been realized via a variety of approaches including multijunction solar cells, quantum dot suspensions, and tandem dye-sensitized photoelectrosynthesis cells. These systems are typically composed of inorganic light-absorbing/charge transport materials (e.g., semiconductors) and often require additional, optically inactive, transition-metal catalysts to perform the bond-breaking/making reactions. Molecule-based, multiphoton harvesting catalytic schemes have been reported but many rely on light-harvesting arrays, redox mediators, or consecutive excitation events (i.e., not

independent chromophores), $^{17-21}$ There are some examples of systems with two independent light-absorbing species enabling artificial Z-schemes for generating long-lived charge separated states, 22 as well as ring expansion, dehalogenation, and detosylation reactions. 23,24 However, a molecular Z-scheme with two independent light-harvesting species that can generate solar fuels like H_2 , in the absence of a co-catalyst, is yet to be realized.

Here, we introduce a system where upon excitation of both a photocatalyst (PC) and an aryl alcohol (ROH) in the presence of a sacrificial electron donor and a proton source, photocatalytic generation of H₂ is achieved (Figure 1, right). In the proposed, dual catalytic cycle, PC is excited and then reduced by a sacrificial electron donor, forming PC⁻ (PC* + $e^- \rightarrow$ PC-). PC- transfers an electron to the photoexcited ROH, followed by the production of H_2 (2PC⁻ + 2ROH* \rightarrow 2PC + 2RO⁻+ H₂). ROH is then regenerated using a proton source, such as phenol (RO⁻ + PhOH → ROH + PhO⁻). Direct electron transfer between PC- and ROH* removes the need for redox mediators. Likewise, hydrogen production directly from the reduction of the aryl alcohol eliminates the need for a secondary H2 producing catalyst. The additive energetics of two independent excitation events also circumvents the thermodynamic constraints associated with the reduction of

Received: August 11, 2022 Published: November 17, 2022





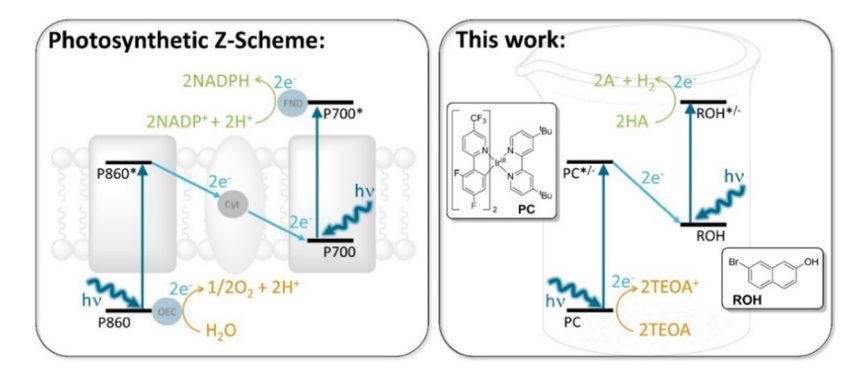


Figure 1. Simplified depiction of the natural photosynthetic Z-scheme (left) and the molecular Z-scheme reported here (right). TEOA = triethanolamine, HA = weak acid.

Table 1. Summary of Various Reaction Conditions and the Resulting Quantity of H₂^a

	reaction condition					product outcome		
entry	[PC] (mM)	[ROH](mM)	[TEOA](mM)	light ^b	other	mmol H ₂ ^c	TON _{PC} ^d	TON_{ROH}^{e}
1	2.5	100	150	UV LED		0.20	5.7	0.1_{4}
2	2.5	100	150	blue LED		0	0	0
3	2.5	100	150			0	0	0
4	2.5	100		UV LED		0	0	0
5		100	150	UV LED		0	0	0
6	2.5		150	UV LED		0.02	0.6	N/A
7	2.5	10	150	UV LED	100 mM PhOH	1.63	46.6	11.6
8	2.5		150	UV LED	100 mM PhOH	0.06	1.7	N/A

^aReaction vessel contained 28 mL of acetonitrile and 3.5 mL of N₂ purged headspace. ^b2000 mW 365 nm LED or 1500 mW 455 nm LED. ^cAll reactions performed in at least duplicate and mmol of H₂ are reported with ±5% accuracy. ^dTON with respect to PC. ^eTON with respect to ROH. Irradiation times were 6 h.

weak acids in their ground state, offering a new paradigm for the conversion of light energy into H₂ bond energy.

2. RESULTS

For this molecular Z-scheme system, the aryl alcohol 7-bromo-2-naphthol (ROH) was chosen as one of the chromophores because its long-lived triplet excited state (τ_{ROH^*} = 15 μ s; Figure S1) enables diffusion-limited bimolecular reactions.²⁵ Also, in the ground state, ROH has a relatively high reduction potential ($E_{\text{red}}^{\text{o}} = -1.39 \text{ V}$ vs saturated calomel electrode, SCE in MeCN) and is only weakly acidic (p $K_a = 27.9$ in MeCN) such that it is unfavorable for ground-state reduction of ROH to RO and H₂ by common photoreduction catalysts (see the SI for more details). The weak acidity of ROH also means the conjugate base RO⁻ will allow for the regeneration of ROH via a weak proton donor (vida infra). Ir(dF-CF₃-ppy)₂(dtbpy)⁺, where dF-CF₃-ppy is 2-(2,4-difluorophenyl)-5-(trifluoromethyl)pyridine and dtpby is 4,4'-tertbutyl-2,2'bipyridine, was chosen as the second chromophore (i.e., photocatalyst; herein PC) because it has a long triplet excitedstate lifetime ($\tau_{PC^*} = 2.2 \ \mu s$; Figure S2) and an excited-state oxidation potential that is thermodynamically below the reduction potential of the ground state of ROH.²⁶ Triethanolamine (TEOA) was used as the sacrificial electron donor because its potential is favorable for the reduction of ³PC* but not ³ROH*.

With system design in hand, irradiation of an MeCN solution containing 100 mM ROH, 150 mM TEOA, and 2.5 mol % PC (0.07 mmol) for 6 h with a 365 nm light-emitting diode (LED) resulted in 0.20 mmol of H₂ corresponding to a turnover number (TON) of 5.7 and 0.1 for the PC and ROH,

respectively. Increasing the irradiation time to 12 h led to a total of 0.3 mmol of H₂. It is also worth noting that with these reaction conditions, no ROH regeneration mechanism was introduced; thus, the maximum theoretical TON with respect to ROH is 1.0 (i.e., 1.4 mmol H_2). While these initial TONs are modest, the results confirm the ability of the system to photocatalytically produce H₂ without the need for an additional transition-metal catalyst to promote the hydrogenbond-making reaction.²⁷

To investigate the mechanism of this reaction, a series of control experiments were performed, and the results are summarized in Table 1. Given the absorption profiles of the chromophores (Figures S3-S5), three different light conditions were used: (1) a 365 nm UV LED capable of exciting both PC and ROH, (2) a 455 nm blue LED that can excite PC but not ROH, and (3) in the dark where no photoexcitation is occurring. Emission profiles for the LEDs can be found in Figure S6. It is worth noting that while 365 nm is not the ideal wavelength for exciting ROH ($\lambda_{max} = 335$ nm), the emission profile for the 365 nm LED overlaps with the low-energy absorption shoulder and has previously been used as an excitation source for ROH.²⁸ Comparing between the irradiation conditions (entries 1-3), a measurable quantity of H₂ was only observed with the UV light source capable of exciting both the PC and ROH (entry 1, Table 1). The lack of H₂ generation under blue light (entry 2) and in the dark (entry 3) suggests that both the PC and ROH must be excited for the reaction to occur.

Further control reactions show the removal of TEOA (entry 4) or PC (entry 5) resulted in no detectable quantities of H₂. A small, but measurable, amount of H₂ was produced from a

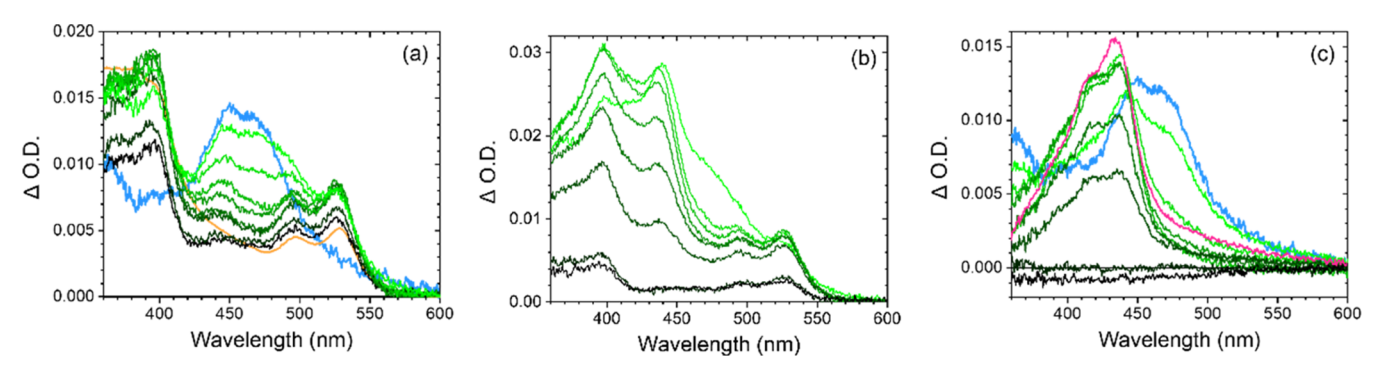


Figure 2. Transient absorption spectra of (a) PC and TEOA (1:10; $\lambda_{ex} = 375$ nm) with $^3PC^*$ (at 5 ns) in blue and the chemically generated PC⁻ spectrum in orange; (b) PC, TEOA, and ROH (1:20:10; $\lambda_{ex} = 335$ nm); and (c) PC and ROH (1:10; $\lambda_{ex} = 375$ nm) with $^3PC^*$ and $^3ROH^*$ (at 5 ns) in blue and red, respectively, in N₂-deaerated MeCN. Time slices progress from green to black at 0.005, 0.5, 1.0, 2.0, 5.0, 10.0, 100, and 1000 μ s.

solution containing just PC and TEOA (i.e., without ROH, entry 6). This H₂ production most likely resulted from the chemical decomposition of oxidized TEOA, as has been previously reported.²⁹ Regardless, the amount of H₂ from TEOA is relatively small compared to that produced from the solution containing ROH (entry 1).

At this point, we envisioned two possible pathways for the photocatalytic generation of H_2 from this system: the reduction of ROH* by PC⁻ to generate H_2 (eq 1) or the generation of acidic protons by ROH* (eq 2) that are then reduced by PC⁻ (eq 3).

$$2ROH^* + 2PC^- \rightarrow H_2 + 2RO^- + PC$$
 (1)

$$2ROH^* \rightarrow 2RO^- + 2H^+ \tag{2}$$

$$2H^+ + 2e^- \rightarrow H_2 \tag{3}$$

To test the proposed mechanisms, we first investigated the redox chemistry of ROH and PC, and then the role of acidity in H₂ generation. PC⁻ was synthesized by chemical reduction with potassium and then added to a solution of ROH in acetonitrile. This solution mixture was stirred in the dark for 6 h, and GC analysis of the solution headspace showed no H₂ production (Table S1). This result indicates that PC⁻ does not reduce ground-state ROH or produce H2 directly. Conversely, a stirred solution of PC- and ROH in acetonitrile under irradiation for 6 h resulted in H_2 production (TON_{ROH} = 0.3, Table S1). This result indicates that ROH must first access its excited state, ROH*, before H2 production occurs when in the presence of PC-. Electrochemical measurements using an indium tin oxide electrode modified with PC³⁰ under reducing bias (-0.4 V vs SCE) gave minimal photocurrent response (<10 μ A) (Figure S7). Upon the addition of ROH, however, switchable photocurrents of >15 μ A were observed, indicating that ROH* can serve as an electron transfer relay in the electrolyte solution. Collectively, these results suggest that the formation of PC⁻ and ROH* is necessary for H₂ production in this catalytic system.

While the above observations are fully consistent with eq 1, they do not rule out the possibility of the mechanism proposed in eqs 2 and 3. Naphthol and its derivatives are known transient photoacids with notably increased acidities in the excited state.³¹ Following excitation and ³ROH* formation, the p K_a of ROH decreases from 27.9 (in MeCN) to 16.4 as determined from a Förster cycle analysis (see the Supporting Information, SI for details).^{32–34} This transient acidity

increases the H⁺ concentration in solution (eq 2), which could be followed by the reduction of H^+ to H_2 (eq 3). However, it is worth noting that the reduction of the solvated proton (i.e., $H^+ + e^- \rightarrow H^{\bullet}$), in the absence of a catalytic electrode such as platinum, has been determined to be -1.96 Vvs SCE^{35,36} and is thus thermodynamically inaccessible in our catalytic system. Nonetheless, to test the role of solution acidity in H2 production and the possible mechanism of eqs 2 and 3, chloroacetic acid (MCA, $pK_a = 15.3$) was used as a surrogate for ³ROH*. Under the standard reaction conditions, 0.07 mmol of H₂ was produced from 100 mM MCA (Table S1), which is nearly 3-fold lower than the solution containing ROH (Table 1, entry 1). It is important to note that the effective concentration of ³ROH* is <0.1 mM because it is limited by photon flux and the excited-state lifetime, and thus the H⁺ concentration for a solution containing 100 mM ROH is at least 3 orders of magnitude lower than for 100 mM MCA. Consequently, the low H₂ production from MCA indicates that the acidity of ³ROH* plays a minimal role in H₂ production from the catalytic solution; thus eqs 2 and 3 are not the likely mechanism for this catalytic system.

To further investigate the H₂ generation mechanism, we performed the direct reduction of ROH electrochemically. Cyclic voltammetry of a 1 mM solution of ROH in acetonitrile (Figure S8) showed an irreversible reduction with an E_n of −1.57 V vs saturated calomel electrode (SCE). This potential is 0.20 V more negative than the oxidation potential of PC-(-1.37 V vs SCE), indicating that PC⁻ should not be thermodynamically capable of reducing ground-state ROH. It is worth noting that the measured E_p includes the common overpotential associated with the reduction of weak acids at carbon electrodes,³⁷ but is in agreement with the lack of H₂ production from PC- and ROH in the dark. Controlled potential electrolysis at -1.60 V vs SCE performed on solutions of various ROH concentrations all led to measurable H_2 production, which scaled linearly with [ROH]² (Figure S9). This is consistent with a second-order reaction with respect to ROH. Electrochemical reduction of ROH was also monitored with UV-visible absorption spectra, and an isosbestic point for the conversion of ROH to RO⁻ (Figure S10) was observed. This is notable for two reasons. First, once ROH is reduced, either electrochemically or via reductive quenching of ROH* by PC-, H₂ is produced concurrently with the conjugate base, RO-. Second, in contrast to 6-bromo-2-naphthol that is known to undergo decomposition via dehalogenation and a 6-carbene

intermediate,³⁸ we observe no side products with ROH (7-bromo-naphthol).

Next, the roles of PC, ROH, and TEOA were investigated using transient absorption spectroscopy (TA), and the results are shown in Figure 2 and the Supporting Information. Two different excitation wavelengths were used: 375 nm for the selective excitation of PC and 335 nm for the excitation of both PC and ROH (Figure S11). For an MeCN solution containing only ROH and TEOA (Figure S12) under 335 nm excitation, the excited-state decay of ³ROH* was the same as in the absence of TEOA ($\tau \approx 15 \ \mu s$). This result shows that TEOA is unable to reductively quench ³ROH*. Conversely, an MeCN solution containing just PC and TEOA showed a rapid (<1 μ s) decrease in the ${}^{3}PC^{*}$ feature (425–500 nm, Figure 2a) upon 375 nm excitation, followed by the formation of structured absorption spectra resembling that of the PCgenerated via chemical reduction. This outcome is consistent with the previously reported reductive quenching reaction, $^{3}PC^{*} + TEOA \rightarrow PC^{-} + TEOA^{+}$, that occurs with a Stern-Volmer quenching rate constant of $6.9 \times 10^8 \text{ M}^{-1} \text{ s}^{-1}$ (Figure S13).²⁶ The resulting PC⁻ lifetime is significantly longer than our acquisition time window (>1 ms).

In a solution containing all three components—PC, ROH, and TEOA—335 nm excitation was followed by the rapid disappearance of the 3 PC* feature (425–500 nm) in <1 μ s, and longer-lived signatures for PC⁻ and 3 ROH* (Figure 2b). Concomitant decay for PC⁻ and 3 ROH* at 420, 440, and 470 nm occurred with a lifetime of \sim 10 μ s (Figure S14), which is faster than the intrinsic decay of PC⁻ (τ > 1 ms) and 3 ROH* ($\tau \approx 15 \,\mu$ s), suggesting a cooperative decay mechanism. Based on the results above, we attribute this cooperative decay to the reduction of 3 ROH* by PC⁻. We observed no spectral features indicative of ROH* formation, which is consistent with the electrochemical reduction of ROH, where H₂ generation was the rapid step.

Unfortunately, due to the inherent instability of PC- and spectral overlap for ROH and PC, we were unable to perform concentration-dependent quenching studies for ³ROH* by PC⁻. However, as a surrogate, we chose to use ferrocene (Fc) as an electron donor (0.4 V vs SCE). Ferrocene is a much weaker reductant than PC- (-1.37 V vs SCE) but has sufficient potential to reduce ³ROH* (1.27 V vs SCE, vida infra). As shown in Figure S15, the excited-state quenching ³ROH* by Fc occurs with a Stern-Volmer rate constant of 2.3 × 10⁹ M⁻¹ s⁻¹. A similar spectral evolution and Stern–Volmer rate constant (2.5 \times 10⁹ M^{-1} s⁻¹; Figure S16) was obtained for the quenching of 2-bromo-7-methoxynaphthalene (ROMe), which has a chromophoric core that is analogous to ROH, but it cannot directly undergo proton reduction. The similarity in spectral evolution and rate constant ($\sim 2.4 \times 10^9 \text{ M}^{-1} \text{ s}^{-1}$) for the quenching of ROH and ROMe suggests that the chromophoric naphthalene units of ROH and ROMe are the likely sites of excited-state reduction. Consistent with previous reports,³⁹ no spectral features were observed for Fc⁺ due to its low extinction coefficient (ε < 500 M⁻¹ cm⁻¹ at 620 nm). However, further support for a reductive quenching mechanism is provided by the fact that a 6 h irradiation of a mixture of 100 mM ROH and 100 mM Fc with a 365 nm LED resulted in the production of 0.20 mmol of H₂.

In an acetonitrile solution containing just PC and ROH, excitation of PC at 375 nm resulted in a TA spectral shift consistent with the ³PC* to ROH triplet energy transfer (Figure 2c) with a Stern–Volmer quenching rate constant of

 $8.0 \times 10^9~{\rm M}^{-1}~{\rm s}^{-1}$ (Figure S17). Importantly, in Figure 2c, there are no indications of the formation of PC⁺/PC⁻ or an increased rate of ³ROH* decay (375–475 nm), demonstrating that no redox events are occurring and ³PC*-to-ROH energy transfer is the only excited-state interaction upon 375 nm excitation. Irradiation of PC and ROH with 335 nm light (Figure S18) resulted in a similar ³PC* to ³ROH* spectral evolution, but with a larger initial contribution from ³ROH* ($\lambda_{\rm max} \approx 440~{\rm nm}$) from direct excitation of ROH. Interestingly, although this triplet sensitization mechanism is competitive with the formation of PC⁻, it is still a productive pathway as it also generates the reactive ³ROH* species.

As described above, irradiation of a solution containing PC, ROH, and TEOA results in the photocatalytic production of $\rm H_2$ and RO $^-$. That reaction, however, is only catalytic with respect to PC, and not ROH, and will stop when ROH is consumed. To regenerate ROH during the catalytic reaction, phenol (PhOH) was added as a sacrificial proton source. The p $K_{\rm a}$ values of PhOH and ROH in MeCN are 27.2 and 27.9, respectively. Consequently, the acid—base equilibrium constant (eq 4) indicates that PhOH-to-RO $^-$ proton transfer is favorable.

$$RO^{-} + PhOH \Rightarrow ROH + PhO^{-}, K_{eq} = 5.0$$
 (4)

Furthermore, ¹H NMR spectra of a solution containing RO⁻ and PhOH shows the formation of ROH and confirms that PhOH can protonate RO⁻ (Figures S19–S21). This regeneration step closes the catalytic cycle with respect to ROH.

To explore the regenerative role of PhOH in the catalytic cycle, an acetonitrile solution containing 2.5 mM PC, 10 mM ROH, 100 mM PhOH, and 150 mM TEOA was irradiated with a 365 nm for 6 h. This reaction resulted in the formation of 1.6 mmol of H₂, which corresponds to a TON of 46.6 with respect to the PC and 11.6 with respect to ROH (Table 1, entry 7). Based on the intensity of the light source (2000 mW), the quantum yield of this reaction is ~5%. Removal of ROH from the reaction (Table 1, entry 8) resulted in a nearly 20-fold decrease in H2, indicating that PhOH is not solely responsible for the observed H₂ increase, and ³ROH* is needed for the observed H₂ production. It is worth noting that the regeneration of ROH from RO- may also prevent homoconjugation between ROH and its conjugate base (RO-...H-OR), an interaction that is known to impede catalytic H₂ generation. 40,41

3. DISCUSSION

Many of the above results can be rationalized by the energy-level diagram depicted in Figure 3. It is energetically favorable for ${}^3PC^*$ to be reduced by TEOA to generate $PC^-([1]$ in Figure 3) and ${}^3ROH^*$ to be reduced by $PC^-[2]$. Reduction of ${}^3ROH^*$ can lead to a bimolecular reaction that generates H_2 and $RO^-[3]$. Electron transfer events 3–7 in Figure 3 are thermodynamically unfavorable and were not observed in any of the control experiments. Of particular note is that while the thermodynamic potential for the reduction of ROH is close to the oxidation potential of PC^- , we did not observe any electron transfer events between PC^- and ground-state ROH.

Accounting for the thermodynamic considerations, we propose Figure 4 as the mechanism for the photocatalytic production of H_2 from a solution of PC, ROH, TEOA, and PhOH. Each step is supported by spectroscopic and electro-

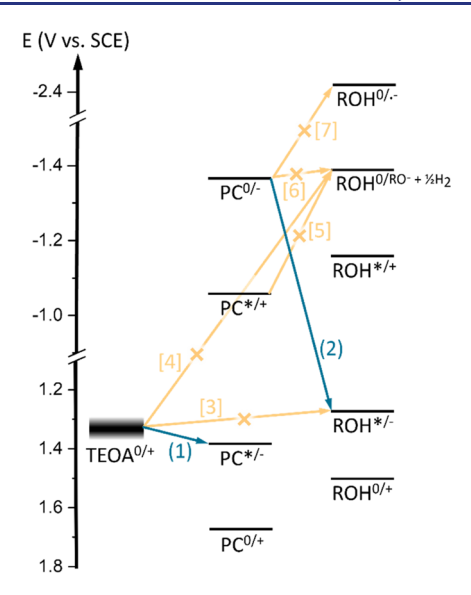


Figure 3. Energy-level diagram for TEOA, PC, and ROH with energetically favorable and unfavorable processes depicted by blue and orange arrows, respectively. Excited-state potentials are for triplet excited states (i.e., ³PC* and ³ROH*).

chemical experiments described in the Results section. This mechanism generates H₂ from the relatively unreactive TEOA and PhOH (PhOH + TEOA $\rightarrow 1/2H_2 + PhO^- + TEOA^+$), which is a thermodynamically unfavorable process by 511 kJ

Steps 1 and 2, the photoexcitation of PC and reduction of PC* by TEOA, have been previously reported²⁹ and are consistent with TA data reported in Figure 2a. These two steps generate the reductant PC-in situ, which has an oxidation potential of -1.37 V vs SCE in acetonitrile. ²⁶ Concurrently, ³ROH* can be generated through either direct excitation with 335 nm light (step 3 in Figure 4, data shown in Figure S1) or triplet energy transfer from ³PC* to ROH (step 4 in Figure 4, data shown in Figure 2c). This energy transfer step effectively makes this a tricatalytic reaction solution (vida infra), but with the sensitization process being redundant and less efficient than direct excitation of ROH. In fact, irradiation with 455 nm blue light, which only directly excites the PC and not ROH, did not result in a measurable quantity of H₂. However, with sufficient blue photon flux, we anticipate that H₂ generation could occur via the ³PC* to ROH triplet sensitization step, but with low quantum yields.

Support for steps 5 and 6 comes from the control reactions where PC- and ROH were mixed in solution. Under dark conditions, no reaction was observed between PC- and ROH, and no H2 was liberated. In contrast, when ROH is excited in the presence of PC-, or a weaker donor like ferrocene, H2 formation is observed (Table 1). This result, and the thermodynamic redox potentials in Figure 3, indicate that photoexcitation of ROH is necessary for electron transfer to occur (step 5 in Figure 4) and either PC or Fc can act as a reducing agent for ³ROH*. Furthermore, the comparable Stern-Volmer rate constant ($\sim 2.4 \times 10^9 \text{ M}^{-1} \text{ s}^{-1}$) for the quenching of ROH and ROMe by Fc suggests that the chromophoric naphthalene units of ROH and ROMe are the likely sites of excited-state reduction by PC⁻ or Fc. In contrast, TEOA is not capable of reducing ³ROH* as shown by TA data (Figure S12), and this is further supported by the lack of H₂ formation when solutions containing only ROH and TEOA were irradiated with 365 nm light (Table 1, entry 5).

Reduction of ³ROH* by PC⁻ results in the formation of H₂ and RO⁻ as depicted in step 6 of Figure 4. The thermodynamic potential for the hydrogen-evolving reduction of ROH at an electrode (i.e., ROH + $e^- \rightarrow RO^- + 1/2 H_2$) is -1.39 V vs SCE, and this value is dictated by the pK_a of ROH.³⁷ Under the experimental conditions here, electrocatalytic H₂ generation was observed at -1.6 V vs SCE (Figure S8) due to the overpotential associated with the reduction of the proton at the surface of the electrode as predicted by Sabtier's principle.⁴² Under these conditions, H2 generation occurs via the reduction of protons on an electrode at potentials lower than one would expect for the direct reduction of ROH to ROH •- (ROH + e- \rightarrow ROH $^{\bullet-}$). However, in the photocatalytic system reported here, no electrodes/catalytic surfaces are present and direct reduction of protons in solution is thermodynamically unfavorable. Consequently, we propose PC⁻ + ³ROH* → $PC + ROH^{\bullet -} \rightarrow RO^{-} + 1/2H_{2}$ as a new and previously unexplored route for H2 production. This proposed H2 evolving mechanism agrees with the experimental data above and is further supported by the following thermodynamic arguments.

As discussed above, the direct ionization of the RO-H bond followed by the reduction of the protons at the electrode surface has a calculated reduction potential of -1.39 V vs SCE. This chemical reaction at the electrode surface supersedes direct reduction of ROH (i.e., ROH + $e^- \rightarrow ROH^{\bullet -}$); therefore, the reduction potential of ROH cannot be directly measured with electrochemical techniques. Instead, ROMe can

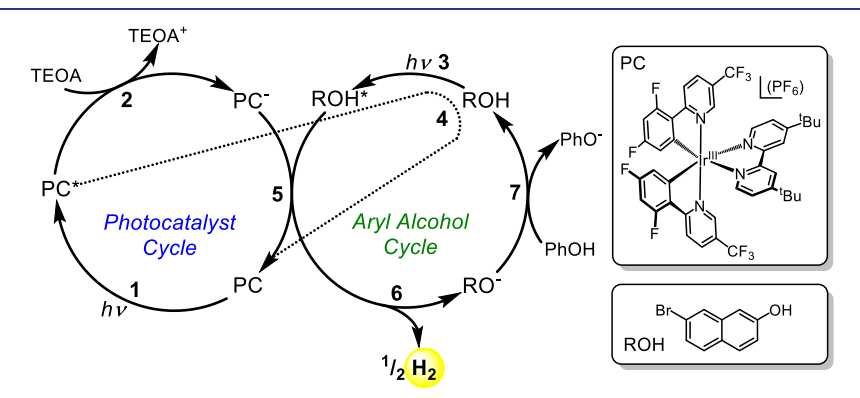


Figure 4. Proposed mechanism for the photocatalytic generation of H₂ from PhOH and TEOA in a molecular Z-scheme consisting of two independent light absorption cycles.

be used as a nonacidic surrogate in which no preceding chemical reactions will interfere with measuring the reduction potential of the naphthol moiety. We can thus estimate the value for the direct reduction of ROH from the $E_{\rm p}$ for ROMe + e⁻ \rightarrow ROMe^{•-}, which is -2.46 V vs SCE (Figure S8). This is likely a high-end estimate by several hundred millivolts due to the electron-donating nature of -OMe relative to -OH likely leading to a more negative reduction potential. Given the E_{0-0} of ${}^3{\rm ROH}^*$ is 2.66 V (see the SI for details), the excited-state reduction potential (${}^3{\rm ROH}^* + {\rm e}^- \rightarrow {\rm ROH}^{\bullet-}$) is calculated to be \geq 0.2 V vs SCE. The net proposed redox reaction that leads to H₂ evolution is thus composed of the two half-reactions shown in eqs 5 and 6.

$$PC^{-} \rightarrow PC + e^{-}, \quad E^{\circ} = 1.37 \text{ V vs SCE}$$
 (5)

$${}^{3}\text{ROH}^{*} + e^{-} \rightarrow \text{ROH}^{\bullet -}, \quad E = 0.2 \text{ V vs SCE}$$
 (6)

$$PC^- + {}^3ROH^* \rightarrow ROH^{\bullet -} + PC, \quad E = 1.57 \text{ V vs SCE}$$
(7)

The direct reduction of ³ROH* at the chromophoric naphthalene core by PC⁻ is thus favorable by $\Delta G = -36.2$ kcal mol-1. Upon the generation of ROH •-, it is thermodynamically downhill for the generation of H₂ as evidenced by the hydrogen evolution potential being roughly 1.0 eV more favorable than the direct reduction of ROH to form ROH $^{\bullet-}$ (-2.46 V for ROH + $e^- \rightarrow ROH^{\bullet-}$ versus -1.39 V for ROH + $e^- \rightarrow RO^- + 1/2 H_2$). Presumably, H_2 generation occurs via a bimolecular reaction between two ROH on molecules that generates H₂ and two RO molecules, which are the only observed products in the reaction mixture. Collectively, the evidence suggests that ³ROH* is acting as an electron acceptor/shuttle, which then directly facilitates H₂ formation without the need of a co-catalyst. This observation opens interesting opportunities for aryl alcohol molecules to serve as chemical, electrochemical, and/or photochemical

It is worth noting that the catalytic production of H₂ from excitation of a brominated naphthol-containing solution was previously observed.³³ In that report, the authors proposed that H_2 generation was initiated by excited-state proton transfer from 6-bromo-2-naphthol to the well-known cobalt-diglyoxime, H_2 generation catalyst. They noted, however, that the measured rate constant $(4.7 \times 10^9 \text{ M}^{-1} \text{ s}^{-1})$ for photoinduced protonation of the cobalt catalyst by 6-bromo-2naphthol, as measured by excited-state quenching of the aryl alcohol, was at least 3 orders of magnitude faster than previously reported rate constants (<10⁶ M⁻¹ s⁻¹) that were measured using stronger ground-state acids.^{43–45} Interestingly, the rate constant for the excited-state quenching of 6-bromo-2naphthol by cobalt-diglyoxime $(4.7 \times 10^9 \text{ M}^{-1} \text{ s}^{-1})$ is in reasonable agreement with the quenching rate constant for 7bromo-2-naphthol by Fc $(2.3 \times 10^9 \text{ M}^{-1} \text{ s}^{-1})$ reported here. In the latter, Fc cannot act as a proton acceptor and H₂ generation catalyst. Given that cobalt-diglyoxime ($E_{1/2} \approx$ -0.5 V vs SCE) is a stronger reductant than Fc ($E_{1/2} \approx 0.4 \text{ V}$ vs SCE), excited-state quenching of 6-bromo-2-naphthol via reduction by Co¹-diglyoxime, followed by H₂ generation from the aryl alcohol, may have been an operable reaction mechanism in that system.

Regarding steps 6 and 7, the formation of RO⁻ from the reduction of ROH is supported by spectroelectrochemical data (Figure S10), which exhibits an isosbestic point with spectral

signatures for ROH and RO⁻. An NMR spectrum collected after a controlled potential electrolysis of ROH was performed also shows the direct formation of RO⁻. The regeneration of ROH by proton transfer from phenol to RO⁻ is supported by NMR studies (Figures S19–S21), where mixing RO⁻ and PhOH results in the formation of ROH and PhO⁻. Regeneration of ROH closes the aryl alcohol cycle and completes the dual catalytic scheme. Further evidence for the complete cycle is given by the NMR spectrum of the post-reaction solution (Figure S22). The NMR spectrum shows the formation of RO⁻, and signals for PC, which match a previous report,²⁹ and indicate molecular stability of the PC (i.e., no ligand loss and protonation of the iridium center).

The net reaction of this mechanism generates H_2 from TEOA and PhOH (PhOH + TEOA \rightarrow 1/2 H_2 + PhO⁻ + TEOA⁺), which is a thermodynamically unfavorable process by 511 kJ mol⁻¹. This high-energy reaction is enabled by the additive effects of two independent excitation events and highlights the ability of this molecular Z-scheme to drive highenergy bond-forming reactions.

4. CONCLUSIONS

Here, we report the realization of a molecular Z-scheme for the photocatalytic production of H₂. This solar fuel-generating reaction is achieved by concurrent excitation of a molecular photoredox catalyst and a naphthol in the presence of an amine electron donor and a phenol proton source. A series of chemical and electrochemical control reactions support a dual catalytic mechanism that exploits two excited-state electron transfer reactions involving the photocatalyst and aryl alcohol, with the net reaction being the reduction of phenol by triethanolamine to generate H₂. Transient absorption measurements further support this proposed mechanism and give evidence for a third catalytic cycle involving triplet energy transfer from the photocatalyst to the aryl alcohol. Despite the modest quantum yield of ~5% for the photocatalytic production of H₂, this entirely molecular artificial Z-scheme can drive a reaction that is uphill by 511 kJ mol⁻¹, thus illustrating the advantages of utilizing simple aryl alcohols for light absorption and catalytic reactivity. The quantum yield of this reaction is also likely limited by the diffusional aspect of the system and could be improved in future studies where the PC and ROH could be chemically bound to eliminate the need for diffusional processes or tethered to an electrode surface in a photoelectrochemical system. This system also represents a new paradigm for the use of aryl alcohol photocatalysts for high-energy reactions.

ASSOCIATED CONTENT

Supporting Information

The Supporting Information is available free of charge at https://pubs.acs.org/doi/10.1021/jacs.2c08462.

NMR, IR, and UV—vis spectroscopic characterization of reaction components and mixtures, and further description of experimental procedures (PDF)

AUTHOR INFORMATION

Corresponding Authors

Kenneth Hanson – Department of Chemistry & Biochemistry, Florida State University, Tallahassee, Florida 32306, United States; orcid.org/0000-0001-7219-7808;

Email: hanson@chem.fsu.edu

Aaron K. Vannucci — Department of Chemistry and Biochemistry, University of South Carolina, Columbia, South Carolina 29208, United States; orcid.org/0000-0003-0401-7208; Email: vannucci@mailbox.sc.edu

Authors

- Pooja J. Ayare Department of Chemistry and Biochemistry, University of South Carolina, Columbia, South Carolina 29208, United States
- Noelle Watson Department of Chemistry & Biochemistry, Florida State University, Tallahassee, Florida 32306, United States
- Maizie R. Helton Department of Chemistry and Biochemistry, University of South Carolina, Columbia, South Carolina 29208, United States
- Matthew J. Warner Department of Chemistry and Biochemistry, University of South Carolina, Columbia, South Carolina 29208, United States
- Tristan Dilbeck Department of Chemistry & Biochemistry, Florida State University, Tallahassee, Florida 32306, United States

Complete contact information is available at: https://pubs.acs.org/10.1021/jacs.2c08462

Author Contributions

§P.J.A. and N.W. contributed equally to this work.

Notes

The authors declare no competing financial interest.

ACKNOWLEDGMENTS

This work was partially supported by University of South Carolina Advanced Support for Innovative Research Excellence (ASPIRE-1) Track-1 (A.K.V., M.R.H., and M.J.W.) and the NSF under Grant No. DMR-1752782 (K.H., N.W., and T.D.). TA measurements were performed on a spectrometer supported by the NSF-MRI program (CHE-1919633) and housed in the FSU Department of Chemistry & Biochemistry's Materials Characterization Laboratory (FSU075000MAC).

REFERENCES

- (1) Alstrum-Acevedo, J. H.; Brennaman, M. K.; Meyer, T. J. Chemical Approaches to Artificial Photosynthesis. 2. *Inorg. Chem.* **2005**, *44*, 6802–6827.
- (2) Dogutan, D. K.; Nocera, D. G. Artificial Photosynthesis at Efficiencies Greatly Exceeding That of Natural Photosynthesis. *Acc. Chem. Res.* **2019**, *52*, 3143–3148.
- (3) Zhang, B.; Sun, L. Artificial photosynthesis: opportunities and challenges of molecular catalysts. *Chem. Soc. Rev.* **2019**, 48, 2216–2264.
- (4) Bard, A. J.; Fox, M. A. Artificial Photosynthesis Solar Splitting of Water to Hydrogen and Oxygen. *Acc. Chem. Res.* **1995**, *28*, 141–145.
- (5) Felton, G. A. N.; Mebi, C. A.; Petro, B. J.; Vannucci, A. K.; Evans, D. H.; Glass, R. S.; Lichtenberger, D. L. Review of electrochemical studies of complexes containing the Fe2S2 core characteristic of [FeFe]-hydrogenases including catalysis by these complexes of the reduction of acids to form dihydrogen. *J. Organomet. Chem.* **2009**, *694*, 2681–2699.
- (6) Kranz, C.; Wächtler, M. Characterizing photocatalysts for water splitting: from atoms to bulk and from slow to ultrafast processes. *Chem. Soc. Rev.* **2021**, *50*, 1407–1437.
- (7) Fukuzumi, S.; Lee, Y.-M.; Nam, W. Bioinspired artificial photosynthesis systems. *Tetrahedron* **2020**, *76*, No. 131024.
- (8) McConnell, I.; Li, G.; Brudvig, G. W. Energy Conversion in Natural and Artificial Photosynthesis. *Chem. Biol.* **2010**, *17*, 434–447.

- (9) Maeda, K. Z-Scheme Water Splitting Using Two Different Semiconductor Photocatalysts. *ACS Catal.* **2013**, *3*, 1486–1503.
- (10) Wang, Y.; Suzuki, H.; Xie, J.; Tomita, O.; Martin, D. J.; Higashi, M.; Kong, D.; Abe, R.; Tang, J. Mimicking Natural Photosynthesis: Solar to Renewable H2 Fuel Synthesis by Z-Scheme Water Splitting Systems. *Chem. Rev.* **2018**, *118*, 5201–5241.
- (11) Guo, H.-L.; Du, H.; Jiang, Y.-F.; Jiang, N.; Shen, C.-C.; Zhou, X.; Liu, Y.-N.; Xu, A.-W. Artificial Photosynthetic Z-scheme Photocatalyst for Hydrogen Evolution with High Quantum Efficiency. *J. Phys. Chem. C* **2017**, *121*, 107–114.
- (12) Sakata, Y.; Hayashi, T.; Yasunaga, R.; Yanaga, N.; Imamura, H. Remarkably high apparent quantum yield of the overall photocatalytic H2O splitting achieved by utilizing Zn ion added Ga2O3 prepared using dilute CaCl2 solution. *Chem. Commun.* **2015**, *51*, 12935–12938.
- (13) Yu, Z. B.; Xie, Y. P.; Liu, G.; Lu, G. Q.; Ma, X. L.; Cheng, H.-M. Self-assembled CdS/Au/ZnO heterostructure induced by surface polar charges for efficient photocatalytic hydrogen evolution. *J. Mater. Chem. A* **2013**, *1*, 2773–2776.
- (14) Li, X.; Garlisi, C.; Guan, Q.; Anwer, S.; Al-Ali, K.; Palmisano, G.; Zheng, L. A review of material aspects in developing direct Z-scheme photocatalysts. *Mater. Today* **2021**, *47*, 75–107.
- (15) Yu, Z.; Li, F.; Sun, L. Recent advances in dye-sensitized photoelectrochemical cells for solar hydrogen production based on molecular components. *Energy Environ. Sci.* **2015**, *8*, 760–775.
- (16) Xiang, C.; Weber, A. Z.; Ardo, S.; Berger, A.; Chen, Y.; Coridan, R.; Fountaine, K. T.; Haussener, S.; Hu, S.; Liu, R.; Lewis, N. S.; Modestino, M. A.; Shaner, M. M.; Singh, M. R.; Stevens, J. C.; Sun, K.; Walczak, K. Modeling, Simulation, and Implementation of Solar-Driven Water-Splitting Devices. *Angew. Chem., Int. Ed.* **2016**, 55, 12974—12988.
- (17) Kobayashi, M.; Masaoka, S.; Sakai, K. Photoinduced Hydrogen Evolution from Water by a Simple Platinum(II) Terpyridine Derivative: A Z-Scheme Photosynthesis. *Angew. Chem., Int. Ed.* **2012**, *51*, 7431–7434.
- (18) Ghosh, I.; Ghosh, T.; Bardagi, J. I.; König, B. Reduction of aryl halides by consecutive visible light-induced electron transfer processes. *Science* **2014**, *346*, 725–728.
- (19) Kerzig, C.; Goez, M. Combining energy and electron transfer in a supramolecular environment for the "green" generation and utilization of hydrated electrons through photoredox catalysis. *Chem. Sci.* **2016**, *7*, 3862–3868.
- (20) Connell, T. U.; Fraser, C. L.; Czyz, M. L.; Smith, Z. M.; Hayne, D. J.; Doeven, E. H.; Agugiaro, J.; Wilson, D. J. D.; Adcock, J. L.; Scully, A. D.; Gómez, D. E.; Barnett, N. W.; Polyzos, A.; Francis, P. S. The Tandem Photoredox Catalysis Mechanism of [Ir(ppy)2(dtb-bpy)]+ Enabling Access to Energy Demanding Organic Substrates. *J. Am. Chem. Soc.* **2019**, *141*, 17646–17658.
- (21) Glaser, F.; Kerzig, C.; Wenger, O. S. Multi-Photon Excitation in Photoredox Catalysis: Concepts, Applications, Methods. *Angew. Chem., Int. Ed.* **2020**, *59*, 10266–10284.
- (22) Favereau, L.; Makhal, A.; Pellegrin, Y.; Blart, E.; Petersson, J.; Göransson, E.; Hammarström, L.; Odobel, F. A Molecular Tetrad That Generates a High-Energy Charge-Separated State by Mimicking the Photosynthetic Z-Scheme. *J. Am. Chem. Soc.* **2016**, *138*, 3752–3760.
- (23) Hu, A.; Chen, Y.; Guo, J.-J.; Yu, N.; An, Q.; Zuo, Z. Cerium-Catalyzed Formal Cycloaddition of Cycloalkanols with Alkenes through Dual Photoexcitation. *J. Am. Chem. Soc.* **2018**, *140*, 13580–13585.
- (24) Glaser, F.; Wenger, O. S. Red Light-Based Dual Photoredox Strategy Resembling the Z-Scheme of Natural Photosynthesis. *JACS Au* **2022**, *2*, 1488–1503.
- (25) McClure, D. S.; Blake, N. W.; Hanst, P. L. Singlet-Triplet Absorption Bands in Some Halogen Substituted Aromatic Compounds. *J. Chem. Phys.* **1954**, 22, 255–258.
- (26) Lowry, M. S.; Goldsmith, J. I.; Slinker, J. D.; Rohl, R.; Pascal, R. A.; Malliaras, G. G.; Bernhard, S. Single-Layer Electroluminescent Devices and Photoinduced Hydrogen Production from an Ionic Iridium(III) Complex. *Chem. Mater.* **2005**, *17*, 5712–5719.

- (27) Whittemore, T. J.; Xue, C.; Huang, J.; Gallucci, J. C.; Turro, C. Single-chromophore single-molecule photocatalyst for the production of dihydrogen using low-energy light. *Nat. Chem.* **2020**, *12*, 180–185.
- (28) Das, A.; Banerjee, T.; Hanson, K. Protonation of silylenol ether via excited state proton transfer catalysis. *Chem. Commun.* **2016**, *52*, 1350–1353.
- (29) Paul, A.; Smith, M. D.; Vannucci, A. K. Photoredox-Assisted Reductive Cross-Coupling: Mechanistic Insight into Catalytic Aryl—Alkyl Cross-Couplings. *J. Org. Chem.* **2017**, *82*, 1996—2003.
- (30) Bobo, M. V.; Paul, A.; Robb, A. J.; Arcidiacono, A. M.; Smith, M. D.; Hanson, K.; Vannucci, A. K. Bis-Cyclometalated Iridium Complexes Containing 4,4'-Bis(phosphonomethyl)-2,2'-bipyridine Ligands: Photophysics, Electrochemistry, and High-Voltage Dye-Sensitized Solar Cells. *Inorg. Chem.* **2020**, *59*, 6351–6358.
- (31) Tolbert, L. M.; Solntsev, K. M. Excited-State Proton Transfer: From Constrained Systems to "Super" Photoacids to Superfast Proton Transfer. *Acc. Chem. Res.* **2002**, *35*, 19–27.
- (32) Kütt, A.; Leito, I.; Kaljurand, I.; Sooväli, L.; Vlasov, V. M.; Yagupolskii, L. M.; Koppel, I. A. A Comprehensive Self-Consistent Spectrophotometric Acidity Scale of Neutral Brønsted Acids in Acetonitrile. *J. Org. Chem.* **2006**, *71*, 2829–2838.
- (33) Dempsey, J. L.; Winkler, J. R.; Gray, H. B. Mechanism of H2 Evolution from a Photogenerated Hydridocobaloxime. *J. Am. Chem. Soc.* **2010**, 132, 16774–16776.
- (34) Forster, T. Z. Electrolytic Dissociation of Excited. *Molecules Electrochem.* **1950**, *54*, 531–535.
- (35) Ellis, W. W.; Raebiger, J. W.; Curtis, C. J.; Bruno, J. W.; DuBois, D. L. Hydricities of BzNADH, C5H5Mo(PMe3)(CO)2H, and C5Me5Mo(PMe3)(CO)2H in Acetonitrile. *J. Am. Chem. Soc.* **2004**, 126, 2738–2743.
- (36) Parker, V. D. Homolytic bond (H-A) dissociation free energies in solution. Applications of the standard potential of the (H+/H.bul.) couple. *J. Am. Chem. Soc.* **1992**, *114*, 7458–7462.
- (37) Felton, G. A. N.; Glass, R. S.; Lichtenberger, D. L.; Evans, D. H. Iron-Only Hydrogenase Mimics. Thermodynamic Aspects of the Use of Electrochemistry to Evaluate Catalytic Efficiency for Hydrogen Generation. *Inorg. Chem.* **2007**, *46*, 8098.
- (38) Pretali, L.; Doria, F.; Verga, D.; Profumo, A.; Freccero, M. Photoarylation/Alkylation of Bromonaphthols. *J. Org. Chem.* **2009**, 74, 1034–1041.
- (39) Fukuzumi, S.; Okamoto, K.; Gros, C. P.; Guilard, R. Mechanism of Four-Electron Reduction of Dioxygen to Water by Ferrocene Derivatives in the Presence of Perchloric Acid in Benzonitrile, Catalyzed by Cofacial Dicobalt Porphyrins. *J. Am. Chem. Soc.* **2004**, *126*, 10441–10449.
- (40) Izutsu, K.Acid-Base Dissociation Constants in Dipolar Aprotic Solvents; Blackwell Scientific: Oxford, U.K., 1990.
- (41) Margarit, C. G.; Asimow, N. G.; Thorarinsdottir, A. E.; Costentin, C.; Nocera, D. G. Impactful Role of Cocatalysts on Molecular Electrocatalytic Hydrogen Production. *ACS Catal.* **2021**, *11*, 4561–4567.
- (42) Laursen, A. B.; Varela, A. S.; Dionigi, F.; Fanchiu, H.; Miller, C.; Trinhammer, O. L.; Rossmeisl, J.; Dahl, S. Electrochemical Hydrogen Evolution: Sabatier's Principle and the Volcano Plot. *J. Chem. Educ.* **2012**, *89*, 1595–1599.
- (43) Baffert, C.; Artero, V.; Fontecave, M. Cobaloximes as Functional Models for Hydrogenases. 2. Proton Electroreduction Catalyzed by Difluoroborylbis(dimethylglyoximato)cobalt(II) Complexes in Organic Media. *Inorg. Chem.* **2007**, *46*, 1817–1824.
- (44) Hu, X.; Brunschwig, B. S.; Peters, J. C. Electrocatalytic Hydrogen Evolution at Low Overpotentials by Cobalt Macrocyclic Glyoxime and Tetraimine Complexes. *J. Am. Chem. Soc.* **2007**, *129*, 8988–8998.
- (45) Szajna-Fuller, E.; Bakac, A. Catalytic Generation of Hydrogen with Titanium Citrate and a Macrocyclic Cobalt Complex. *Eur. J. Inorg. Chem.* **2010**, 2010, 2488–2494.

□ Recommended by ACS

 $\label{light-Promoted Radical Cross-Dehydrogenative Coupling of $C(sp^3)$-$H/C(sp^3)$-$H and $C(sp^3)$-$H/C(sp^2)$-$H via Intermolecular HAT$

Xinpeng Xie, Lei Shi, et al.

ORGANIC LETTERS

READ 🗹

Efficient Hydrogen Production by a Photoredox Cascade Catalyst Comprising Dual Photosensitizers and a Transparent Electron Mediator

Nobutaka Yoshimura, Atsushi Kobayashi, et al.

MARCH 13, 2023

JOURNAL OF THE AMERICAN CHEMICAL SOCIETY

READ 🗹

Efficient Red-Light-Driven Hydrogen Evolution with an Anthraquinone Organic Dye

Mei Ming, Zhiji Han, et al.

OCTOBER 19, 2022

JOURNAL OF THE AMERICAN CHEMICAL SOCIETY

READ 🗹

Multi-Electron Visible Light Photoaccumulation on a Dipyridylamine Copper(II)-Polyoxometalate Conjugate Applied to Photocatalytic Generation of CF₃ Radicals

Weixian Wang, Sébastien Blanchard, et al.

MAY 22, 2023

JOURNAL OF THE AMERICAN CHEMICAL SOCIETY

READ 🗹

Get More Suggestions >